Available online at www.sciencedirect.com
ScienceDirect
International Journal of Thermal Sciences 47 (2008) 1602–1609
International Journal of Thermal Sciences
www.elsevier.com/locate/ijts

Atomistic-mesoscale interfacial resistance based thermal analysis of carbon nanotube systems

V.U. Unnikrishnan [a], D. Banerjee [b], J.N. Reddy [a,*]

[a] *Advanced Computational Mechanics Laboratory, Department of Mechanical Engineering, Texas A&M University, College Station, TX 77843-3123, USA*
[b] *Multi Phase Flows and Heat Transfer Laboratory, Department of Mechanical Engineering, Texas A&M University, College Station, TX 77843-3123, USA*

Received 15 May 2007; received in revised form 15 October 2007; accepted 22 October 2007

Available online 10 April 2008

Abstract

This paper estimates the effect of chemical additives like CuO on the interfacial thermal resistance of carbon nanotubes (CNTs) embedded in water. The investigation of thermal properties of CNT nanostructure is carried out using molecular dynamics (MD) simulations. The nanotube was heated to a prescribed temperature, followed by the relaxation of the entire configuration. In the equilibration simulations, the atoms in the nanotube are heated instantaneously to 500, 750 and 1000 K in 3 separate simulations by rescaling the velocities of carbon atoms in the nanotube. This paper also deals with the mesoscale thermo-conductivity properties of the composite system, by employing various effective medium theories and micromechanical methods.
© 2007 Elsevier Masson SAS. All rights reserved.

Keywords: Carbon nanotube; Molecular dynamics; Universal force field potential; Interfacial thermal resistance; Effective medium theories; Thermal conductivity

1. Introduction

Carbon nanotubes (CNTs) are present mainly in three configurations: single-walled carbon nanotubes (SWNT), multi-walled carbon nanotubes (MWNT), and carbon nanotube bundles or ropes. These configurations are many orders of magnitude stronger, stiffer, conductive, and lighter than the best available carbon fibers [1–8]. The perfect formation of nano-unit cells and the ease by which the structural as well as functional units can be manipulated helps in finding exciting structural applications [2]. For the manipulation of nanoscale systems, molecular level study involving interactions at the atomic scale need to be analyzed. The simulation of molecular systems is based on the assumption that the atomic interactions are described by means of classical mechanics models [6,7,9–11]. Studies in the mechanical, electrical and thermal behavior of CNTs were focused primarily on the use of empirical potentials using molecular dynamics (MD) and continuum models using the elasticity theory [6–8,12,13]. Even though MD simulations are popular in the atomistic scale, the computational adaptations to model macroscopic problems based on CNTs are not completely established.

Research in the determination of overall properties of the composite systems are carried out with a bottom to top approach [6,14]. Of late, greater focus is on the accuracy in predicting the lower order properties and hierarchical transfer of the material properties to a larger scale. In the previous works on multiscale modeling, the response in the atomistic level was transferred to the mesoscale or microscale by the explicit use of "equivalence of the response variables" [14]. In the atomistic level the interactions are modeled using pair potentials to respond to externally applied disturbance. The response variables in the lower scales are passed on to the next higher scale, seeking change in the material properties. This method is justified, since the material response at an atomistic scale is highly nonlinear [11] and any change in the local environment has been found to vary the properties of the atomistic system dramatically [6].

Numerous theoretical models predict that an addition of even a low volume fraction of CNTs would result in an increase in thermal conductivity of a composite system [15–17]. Inter-

* Corresponding author. Tel.: +1 979 862 2417; fax: +1 979 845 3081.
E-mail address: jnreddy@tamu.edu (J.N. Reddy).

1290-0729/$ – see front matter © 2007 Elsevier Masson SAS. All rights reserved.
doi:10.1016/j.ijthermalsci.2007.10.012

face thermal resistance in nanocomposites or nanosystems is one of the most important factors that contributed to the large variation in the reported values of thermal conductivities in literature [18]. This discrepancy was found to be due to the weak atomic bonding between the particle and surrounding matrix interface [19,20]. Interface thermal resistance values reported for carbon nanotubes embedded in various materials is found to range from 0.76×10^{-8} to 20.0×10^{-8} m^2 K/W. From the works of Huxtable et al. [20,21] an accepted value of 8.3×10^{-8} m^2 K/W was obtained from numerical and experimental methods [20–22].

Foygel et al. [23] obtained a value of 2.9×10^{-8} m^2 K/W by Monte Carlo simulations, 3.3×10^{-8} m^2 K/W was also reported by Shenogin et al. [15–17,24] using numerical methods. Xue et al. uses 5.0×10^{-8} m^2 K/W for the estimation of effective thermal conductivities for CNT systems [20]. Interfacial thermal resistance values of 6.46×10^{-8} m^2 K/W for SWNT nanoropes were reported by Murayama et al. [22,25] and for neat and functionalized CNTs, Clancy and Gates had reported values of 0.2×10^{-8} to 9.6×10^{-8} m^2 K/W. In one of the recent works by Gao et al. [16] the interfacial thermal resistance value of 1.58×10^{-8} m^2 K/W was derived based on experimental observations for SWNTs. The interfacial resistance values are also found to be dependent on the length of the nanotube and a value of 12.2×10^{-8} m^2 K/W was reported by Murayama et al. [25] using molecular dynamic simulation for very long CNT with entrapped water and 14.4×10^{-8} m^2 K/W was reported by Choi et al. [17,26] for long CNTs.

However, previous works in this area have not been able to capture the variations of the interfacial thermal properties in presence of additives in the solvent phases like CuO, which is the objective of this paper. There have been very few studies on the thermo-physical characteristics of CuO nanoparticles in water [27,28]. Recent studies on the dispersion of CuO in water using novel procedures by ultrasound and microwave irradiation has also shown that there is an enhancement of thermal conductivity of the ensuing CuO aqueous nanofluid [27]. This paper also shows how the change in the interfacial thermal resistance values due to the additives, changes the overall effective thermal conductance of the composite system. The thermal conductivities are estimated using the two effective medium theories that take into consideration the interfacial thermal effects and subsequently comparing this with the lower and upper bounds established using well-known micromechanical methods. All molecular dynamics simulations were performed using Cerius2 (version 4.6, Accelrys, Inc.) simulation package.

The paper is organized as follows. Section 2 describes the analysis procedure for the estimation of thermal and mechanical properties of carbon nanotube systems and a detailed description of the atomistic simulation of CNT and water system using MD simulations is given. The simulation procedure used in this paper is described in Section 3. An outline of the interfacial thermal resistance is given in Section 4. The effective medium theories like Maxwell–Garnett-type effective medium approach, Bruggeman effective medium theory, and the Hashin–Shtrikman bounds are described in Section 5 along with the discussion. The paper concludes with the summary in Section 6.

2. Analysis of single-walled CNT: Molecular dynamics

Single-walled nanotubes are idealized as being formed by the folding of graphene sheet into a hollow cylinder, which is composed of hexagonal carbon ring units referred to as graphene units [6,11,29]. Each of the carbon atoms forming the tubules has three nearest neighboring bonds. In a fully relaxed structure, the angles between these bonds depend on the radius of the cylinder as well as on their orientation [11,29]. All the three angles approach 120° (perfect graphitic plane) with increasing cylindrical radius. The fundamental CNT structure can be classified into three categories: armchair, zigzag, and chiral, in terms of their helicity. One of the advantages of atomistic simulation is the ease with which various configurations can be studied when compared to an experimental investigation of CNT. The experimental investigation is extremely difficult as it is limited by the availability of high quality defect free CNTs of sufficient length and in the measurement of nanoscale objects [30].

Properties of CNTs can be obtained from various experimental investigations, but a thorough understanding of these properties, as in case of any chemical/molecular system, must be obtained by using computational models. These models could be used for parametric study based on the material characteristics, geometric variations and other molecular modifications. Therefore, theoretical investigation of the mechanical properties of the CNTs can also be carried out by these classical methods of analysis for molecular systems. A complete quantum mechanical simulation of the entire molecular structure is computationally prohibitive beyond a few atomic configurations. MD is a computational tool that enables computation of the trajectories of atoms by integrating Newton's second law of motion. It determines the mechanical force field that exists in an atom due to interactions from the surrounding atoms by means of a potential field.

Molecular dynamics has been a very popular tool for the simulation of various atomistic structures for the determination of mechanical, thermal and other properties of interest [31–33]. The thermodynamic state characterized by the fixed number of atoms, volume and temperature called the Canonical Ensemble [33] forms the basis of the molecular dynamic simulation in this work. The simulated system and the heat bath couple to form a composite system. The conservation of the energy still holds in the composite system but the total energy of the simulated system fluctuates. The motion of the particles in the system is governed by the Hamiltonian which is a function of the position and momentum of the particles, and the Hamiltonian equations of motion. The Hamiltonian representing the total energy of an isolated system is given as the sum of the potential, kinetic energy terms and thermodynamic terms as shown in Eq. (1). This can also be represented as the total energy of the system as shown in Eq. (2).

$$H(r^N, p^N) = \frac{1}{2m} \sum_i p_i^2 + U(r^N) \tag{1}$$

$$E(p^N, r^N) = E_k(p^N) + U(r^N) \tag{2}$$

where $U(r^N)$ is the potential energy from intermolecular interactions as a function of the spatial ordinate r^N, $\frac{1}{2m}\sum_i p_i^2$ represents the momentum p of the particle i with mass m_i, which is a function of the absolute temperature called the kinetic energy $E_k(p^N)$ and p^N represents the total momentum of the N particle system. With the time derivative of the Hamiltonian as in Eq. (3), and with the spatial derivative as in Eq. (4), we can obtain the equations of motion [6].

$$\frac{\mathrm{d}H}{\mathrm{d}t} = \frac{1}{m}\sum_i p_i.\dot{p}_i + \sum_i \frac{\partial U}{\partial r_i}.\dot{r}_i = 0 \tag{3}$$

$$\frac{\mathrm{d}H}{\mathrm{d}r_i} = \frac{\partial U}{\partial r_i} \tag{4}$$

The reliability of a molecular dynamics simulation depends mainly on the type of potential functions used. In general, the minimum energy configuration of the CNT is found using the minimization of the potential energy at 0 K and is taken as the initial energy of the system [6]. The total potential energy (E) field can be divided into nonbonded and bonded interactions

$$E = \underbrace{U_{vdW}}_{\text{Nonbonded potential}} + \underbrace{(U_{\text{bond-stretch}} + U_{\text{angle-bend}} + U_{\text{torsion}})}_{\text{Bonded potentials}} \tag{5}$$

The nonbonded interaction is the Lennard-Jones (LJ) "12:6" potential model and is given as

$$U_{vdW}(r_{ij}) = 4k\left[\left(\frac{r_0}{r_{ij}}\right)^{12} - \left(\frac{r_0}{r_{ij}}\right)^{6}\right], \quad r_{ij} \leqslant r_c \tag{6}$$

where (i, j) are the atomic pairs, r_{ij} is the bond distance given by the difference in the position vectors of atoms i and j as $r_{ij} = |\mathbf{r}_i - \mathbf{r}_j|$ and k is a parameter characterizing the interaction strength, r_0 defines a molecular length scale, r_c is the cutoff distance such that $U_{vdW}(r_c) \approx 0$, if $r_{ij} > r_c$. A major part of the total potential energy is the bonded energy, which is the sum of the three different interactions among atoms: bond stretching, angle bending and torsion. The force constants in the potential equations are normally obtained from quantum mechanical (ab-initio) or experimental methods [13,34]. The general-purpose Universal Force Field (UFF) of Cerius[2] (version 4.6, Accelrys, Inc.) is used in the present simulations. The universal force field is based on simple relations having parameters that depend on the type of element, hybridization and connectivities. The UFF includes hybridization-dependent atomic bond radii, hybridization angles, van der Waals parameters, torsional and inversion barriers and effective nuclear charges. The potential energy of a molecule is the result of a series of superposition of various two-bodied, three and four body interactions [35,36].

3. Simulation procedure

A (5, 5) single-walled nanotubes with a diameter of 7 Å immersed in water has been used in the analysis. The simulations are carried out on a CNT with 200 carbon atoms, corresponding to a nanotube length of ∼23.0 nm, and 435 water molecules and the carbon and hydrogen atoms are modeled explicitly (see Fig. 1a). In the simulations the entire systems was minimized and later equilibrated for 1 ps (1000 steps). The temperature scaling was carried out in 10 ps as an NVT ensemble (10 000 steps). During the minimization and NVT processes, the atoms in the periodic unit cell are allowed to equilibrate within the fixed MD cell. Periodic boundary conditions are applied in all directions. To find the effect of CuO additive on the interfacial thermal property, 32 CuO molecules were added to the water system randomly. These were also equilibrated and bought to the required temperature by similar set of thermostat algorithms (see Fig. 1b).

In the molecular dynamic simulations, the interatomic interactions are calculated using a "UFF-Valbond1.1 Molecular Force Field" which includes van der Waals, bond stretch, bond angle bend, and torsional rotation terms [36]. The UFF is well suited for MD simulations as it allows for accurate vibration measurements [37]. UFF is a purely harmonic force field. The UFF has been reported to have full coverage of the periodic table [37] and can be used for predicting the geometries and conformational energy differences of organic molecules etc and can be used for organometallic systems [36,37]. After the en-

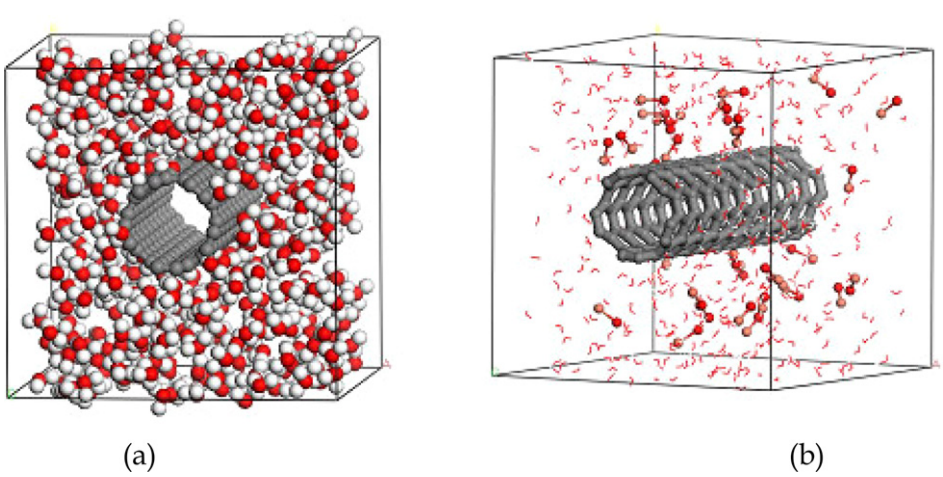

Fig. 1. Initial state of unit cell with SWNT immersed in (a) water only (b) water with CuO additive.

sembles were equilibrated and brought to the required base temperature of 300 K, the temperature of the nanotube was raised to a predefined temperature. This was carried out by a simple rescaling of the velocities of the atoms of the nanotube instantaneously [18,21,24]. Direct velocity scaling changes the velocities of the atoms to result in the target temperature of the ensemble. In this study the following rescaling procedure is used:

$$\left(\frac{v_{\text{new}}}{v_{\text{old}}}\right)^2 = \frac{T_{\text{target}}}{T_{\text{system}}} \tag{7}$$

where T_{target} is the target temperature to scale to, T_{system} is the instantaneous temperature of the system having velocities v_{old} and the final scaled velocity is v_{new} for each atom of the CNT in the configuration. The modified configuration is now allowed to relax under constant energy. The difference in temperature between the atoms of the CNT and the water molecules including the additives are now plotted against the MD time steps.

4. Interfacial thermal resistance

In the equilibration simulations, the atoms in the nanotube are heated instantaneously to 500, 750 and 1000 K by rescaling the velocities of carbon atoms in the nanotube. The system is allowed to relax without any thermostating effects. It is normally seen that the decay of the temperature is of an exponential order [18,24]. This decay of the temperature from the nanotube to the surrounding matrix molecules is limited by the interfacial thermal resistance. The interfacial thermal barrier resistance was first measured by Kapitza in 1941 and this interfacial thermal resistance is generally known as the Kapitza resistance [20, 38]. Under such conditions, the time constant, τ, of the decay depends on the nanotube heat capacity, C_T and the thermal resistance of the nanotube-matrix interface R_k

$$\tau = \frac{R_k C_T}{A_T} \tag{8}$$

where A_T is the area of the nanotube and C_T/A_T is the heat capacity per unit area of the SWNT and is usually taken as 5.6×10^{-4} J/m^2 K [18,21,24].

The cooling profile of the two configurations against the MD time step is shown in Fig. 2 for clean water and in Fig. 3 for the case of water with CuO additive. It can be seen that the temperature profile follows an exponential order as predicted by various researchers [18,24]. The interfacial thermal resistance values for the two systems are shown in Fig. 4. It can be seen that the interfacial thermal resistance values are well within the values given in literature based on the length of the nanotube used in the analysis. It is to be noted that there is a marginal increase in the thermal resistance when the water surrounding the nanotube has CuO additive. This modified thermal resistance values are used to estimation the change in the thermal conductivity of an impure water composite system by using the various effective medium theories [38,39]. Similar analyses were also carried out for DWNTs immersed in water and the initial configuration of the DWNT composite system is shown in Fig. 5. The cooling profile against the MD time step for

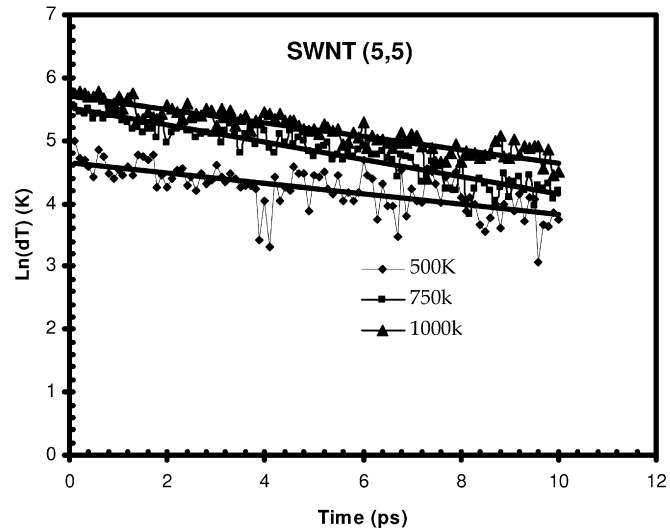

Fig. 2. Cooling profile of SWNT in water.

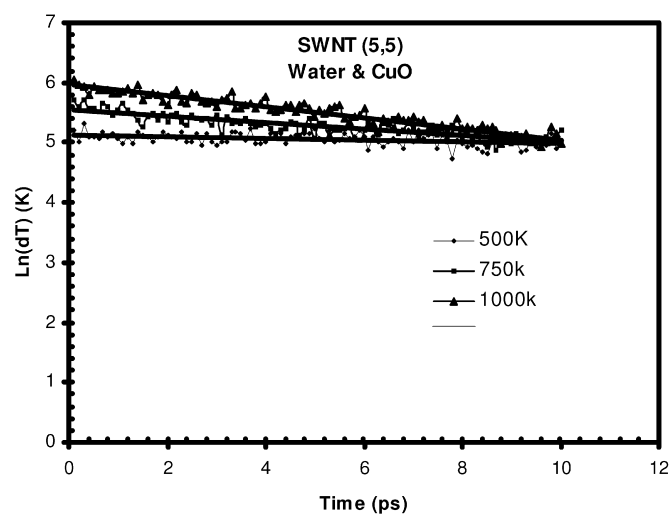

Fig. 3. Cooling profile of SWNT in water with CuO additive.

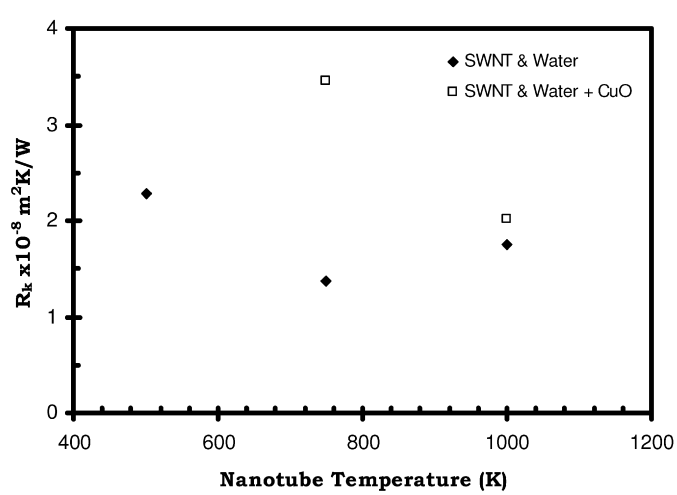

Fig. 4. Interface thermal resistance values of SWNT heated to various temperatures and immersed in pure water and water with CuO additive.

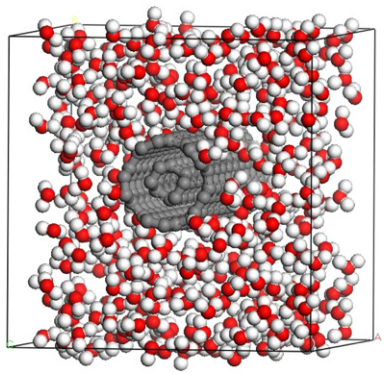

Fig. 5. Initial state of unit cell with DWNT immersed in water.

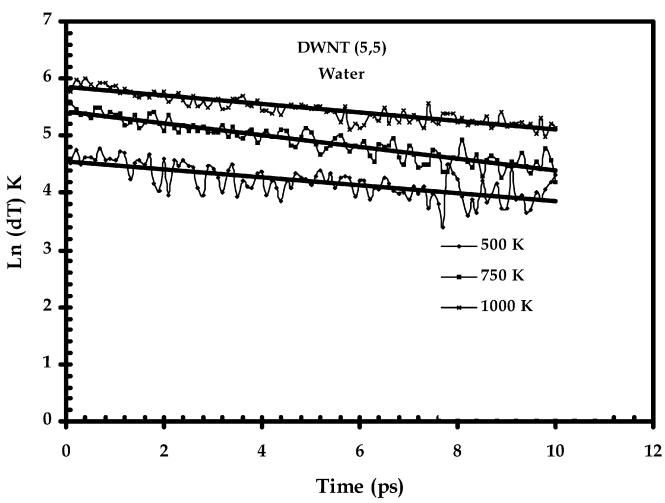

Fig. 6. Cooling profile of DWNT in water.

Table 1
Interface thermal resistance values of DWNT heated to various temperatures and immersed in pure water

CUT temperature (K)	DWNT water $\times 10^{-8}$ m^2 K/W
500	2.6455
750	1.7670
1000	2.4890

DWNT in water is shown in Fig. 6 and the interfacial thermal resistance values for DWNT for various temperatures are given in Table 1.

5. Thermal conductivity of CNT-fluid systems

There is a strong dependence on temperature and material properties on the effective thermal conductivity of a material [18]. Unlike assuming that there exists a perfect bonding between the nanotube and the surrounding materials, there exists an interphase layer which contributes to the interfacial thermal resistance [18,40,41]. This interfacial thermal resistance (R_K) between the constituent phases in a composite is due to a combination of mechanical or chemical bonding at the interface known (see Fig. 7) as the Kapitza radius [20,38]. The effective medium approach has been used to take into consideration this resistance that leads to the determination of the effective thermal property. The effective medium approach is an analytical homogenization tool and is not accurate as a direct atomistic simulation procedure.

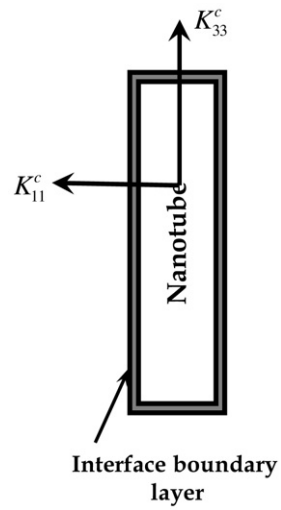

Fig. 7. Composite unit cell of a nanotube coated with a very thin interfacial thermal barrier layer.

5.1. Maxwell–Garnett-type effective medium approach (EMA)

The Maxwell–Garnett-type effective medium approach is assumed to be valid for small volume fractions of CNTs [40, 41]. The thermal conductivity of the fiber phase is also assumed to be larger than that of the matrix phase. The effective thermal conductivity of a nanotube composite system is given by [40, 41]

$$K_e = K_m \frac{3 + v_f(\beta_x + \beta_z)}{2 - v_f \beta_x} \tag{9}$$

with, $\beta_x = \frac{2(K_{11}^c - K_m)}{K_{11}^c + K_m}$ and $\beta_z = K_{33}^c/K_m - 1$ and v_f is the volume fraction of the nanotube fiber phase. K_{11}^c and K_{33}^c are the equivalent thermal conductivities (see Eq. (10)) along transverse and longitudinal axes respectively of a composite unit cell as shown in Fig. 7 and K_m and K_c are the thermal conductivities of the matrix phase and the fiber phase respectively.

$$K_{33}^c = \frac{K_c}{1 + \frac{2a_K}{L}\frac{K_c}{K_m}} \quad \text{and} \quad K_{11}^c = \frac{K_c}{1 + \frac{2a_K}{d}\frac{K_c}{K_m}} \tag{10}$$

where $a_K = R_K K_m$.

The interfacial thermal conductivities of nanotube–water composite systems and with CuO as the added impurity was used for the estimation of the overall effective conductivity. The conductivity of single walled nanotube was taken as 6000 W/mK and of water is taken as 0.6 W/mK [18]. It is assumed that the addition of the impurity is not significant enough to change the effective thermal conductivity of water but changes the interfacial thermal resistance. The effective thermal conductivities can be found to lie between the thermal conductivities from the maximum and minimum reported val-

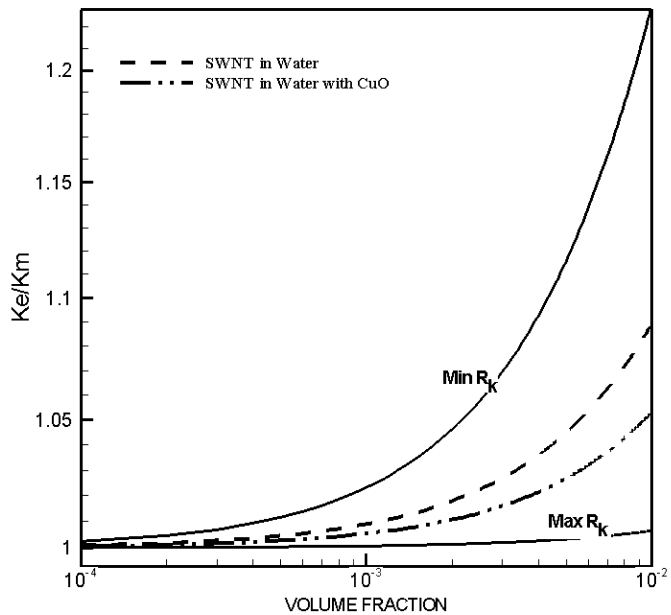

Fig. 8. Effective thermal coefficient of SWNT in pure water and water with CuO additive.

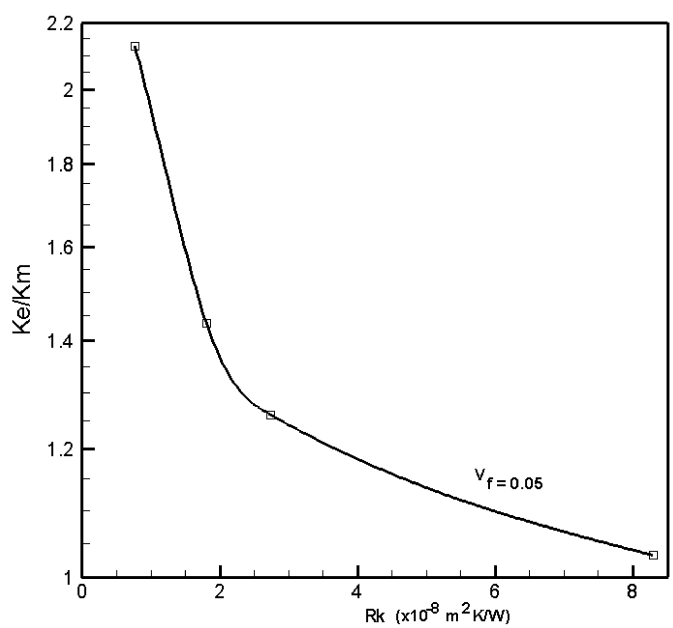

Fig. 9. Variation of effective thermal coefficient with interfacial thermal resistance values for volume fraction 0.05.

ues of the interfacial thermal resistances reported in literature as shown in Fig. 8. The effect of varying interface thermal resistance on the effective thermal conductivity for a fiber volume fraction of 0.05 is shown in Fig. 9, and it can be seen that there is a nonlinear dependence on the change in the thermal conductivity of the nanotube composite structure [41]. The effective thermal conductivities for DWNT based composite systems are shown in Fig. 10 for various fiber phase volume fractions. A widely used thermal conductivity value for MWNT is taken as 3000 W/mK [41].

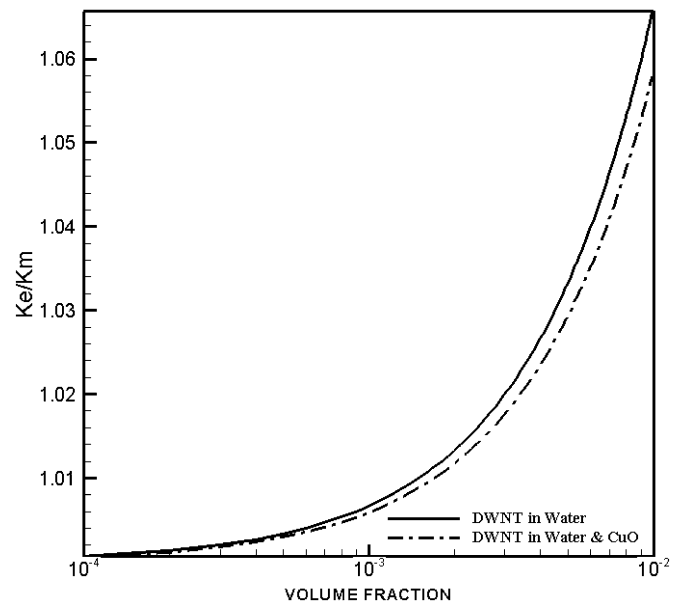

Fig. 10. Effective thermal coefficient of DWNT in pure water and in water with CuO additive.

5.2. Bruggeman effective medium theory (EMT)

In Bruggeman's EMT the effective thermal conductivity for carbon nanotube composites was formulated by using the interface thermal resistance along with an average polarization theory [16,39]. The effect of the length of the nanotube, diameter, volume fraction, and interface thermal resistance on the effective thermal conductivity is taken into consideration in this method. This effective medium theory is able to model the nonlinear dependence of the thermal conductivity on the volume fraction of the fiber phase material. According to this theory, the effective thermal conductance is related to the thermal resistance of the matrix and the fiber phase material and the volume fraction by Eq. (11) [16,39]

$$(1-v_f)\frac{K_e-K_m}{2K_e-K_m}+\frac{v_f}{9}\sum_{j=x,y,z}\frac{K_e-K_{c,j}}{K_e+L_j(K_{c,j}-K_e)}=0 \tag{11}$$

where, the aspect ratio of the nanotube is $P=a/c$, and L_j is the depolarization factor given by Eq. (12), K_m is the thermal conductivity of matrix phase, $K_{c,j}$ is the thermal conductivity of the fiber along j-axis as given in Eq. (13), $R_K = \lim_{\delta\to\infty,\ K_s\to 0}\delta/K_s$ is the interfacial thermal resistance and is obtained from the molecular dynamic simulations and $Q = \frac{(2a+c)}{ac}$

$$L_x=\frac{1}{2(P^2-1)^{3/2}}\left[P\ln\frac{P+\sqrt{P^2-1}}{P-\sqrt{P^2-1}}-2\sqrt{P^2-1}\right]$$

$$L_y=L_z=\frac{1-L_x}{2} \tag{12}$$

$$K_{c,j}=\frac{K_p}{1+QR_KL_jK_p} \tag{13}$$

The effective thermal conductance of the composite material can be obtained by simplifying Eq. (11) through (13) and is given in Eq. (14)

$$9(1-v_f)\frac{K_e-K_m}{2K_e-K_m}+v_f\left[\frac{K_e-K_{c,x}}{K_e+L_x(K_{c,x}-K_e)}+4\frac{K_e-K_{c,y}}{2K_e+(1-L_x)(K_{c,y}-K_e)}\right]=0 \quad (14)$$

5.3. Hashin–Shtrikman (H–S) bounds

The variationally consistent Hashin–Shtrikman bounds are one of the best possible bounds for macroscopically homogeneous, isotropic, two-phase materials that can be derived from the properties of the individual components like volume fraction of the various phases and thermal conductivities. Only a brief description is given in this paper and the readers may refer standard literature on micromechanical analysis [42] for a detailed description of the HS bounds. The Hashin–Shtrikman (H–S) bounds for the thermal conductivity of a two-phase material are given by Eqs. (15) and (16).

$$K_L=K_m+\frac{v_f}{\frac{1}{K_p-K_m}+\frac{(1-v_f)}{3K_m}} \quad (15)$$

$$K_H=K_p+\frac{(1-v_f)}{\frac{1}{K_m-K_p}+\frac{v_f}{3K_m}} \quad (16)$$

where K_L is the H–S lower bound and K_H is the H–S upper bound.

The interfacial thermal conductivities of nanotube–water composite systems and with CuO as the added impurity was also used in the estimation of the overall effective conductivity. The conductivity of single walled nanotube is taken as 6000 W/mK and of water is taken as 0.6 W/mK [18]. The effective thermal conductivities for various interfacial thermal resistances was found to lie between the thermal conductivities from the maximum and minimum reported values of the interfacial thermal resistances reported in literature as shown in Fig. 11, and is also found to lie between the HS bounds.

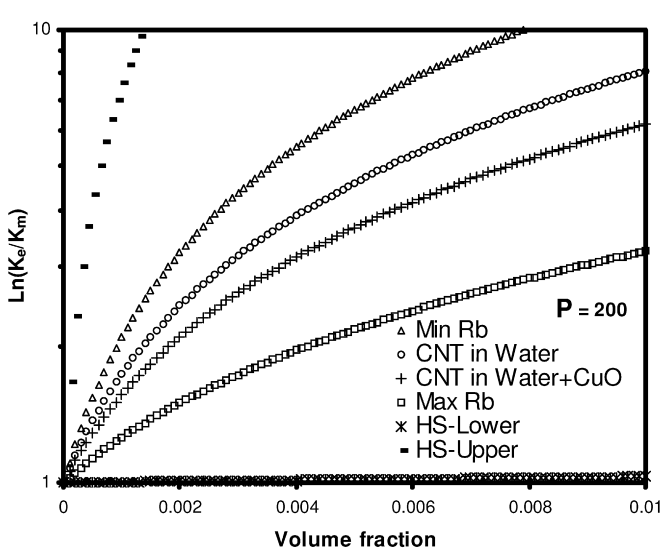

Fig. 11. Effective thermal coefficient of SWNT in pure water and water with CuO additive with bounds (HS—Hashin–Shtrikman lower and upper bounds, min and max Rb—bounds for minimum and maximum reported values of R_b).

6. Conclusions

The thermal conductivity analysis of a nanotube system having pure water and water with CuO additive has been analyzed in this paper. The effect of this admixture on the interfacial thermal resistance has been obtained by molecular dynamic simulation. The obtained interfacial thermal resistance was then applied to various effective medium theories to ascertain the effect on the overall thermal conductance of the composite system. The effective conductivities are found to be bounded by the Hashin–Shtrikman bounds which are established by micromechanical methods.

Acknowledgements

The authors are grateful to the National Science Foundation for supporting this work from grant number NSF-CTS-0630703. The authors are also grateful to the Texas A&M University's Super Computing Facility for providing the computational support and the Laboratory for Molecular Simulation in the Department of Chemistry at Texas A&M University for the software support.

References

[1] S. Iijima, Helical microtubules of graphitic carbon, Nature 354 (6348) (1991) 56–58.
[2] R.H. Baughman, A.A. Zakhidov, W.A. de Heer, Carbon nanotubes—the route toward applications, Science 297 (2002) 787–792.
[3] M.S. Dresselhaus, G. Dresselhaus, P. Eklund, Science of Fullerenes and Carbon Nanotubes: Their Properties and Applications, Academic Press, New York, 1996.
[4] A. Sears, R.C. Batra, Macroscopic properties of carbon nanotubes from molecular-mechanics simulations, Physical Review B (Condensed Matter and Materials Physics) 69 (23) (2004) 235406–235410.
[5] E.T. Thostenson, T.W. Chou, On the elastic properties of carbon nanotube-based composites: modeling and characterization, Journal of Physics D: Applied Physics 36 (5) (2003) 573–582.
[6] V.U. Unnikrishnan, J.N. Reddy, Characteristics of silicon doped carbon nanotube reinforced nanocomposites, International Journal for Multiscale Computational Engineering 3 (4) (2005) 437–450.
[7] B.I. Yakobson, C.J. Brabec, J. Bernholc, Nanomechanics of carbon tubes: Instabilities beyond linear response, Physical Review Letters 76 (14) (1996) 2511–2514.
[8] Q. Zhao, M.B. Nardelli, J. Bernholc, Ultimate strength of carbon nanotubes: A theoretical study, Physical Review B 65 (14) (2002) 144105–144110.
[9] S. Blonski, W. Brostow, J. Kuba't, Molecular-dynamics simulations of stress relaxation in metals and polymers, Physical Review B 49 (10) (1994) 6494–6500.
[10] I. Che, T. Cagın, I.W.A. Goddard, Studies of fullerenes and carbon nanotubes by an extended bond order potential, Nanotechnology 10 (1999) 263–268.
[11] D. Srivastava, C. Wei, K. Cho, Nanomechanics of carbon nanotubes and composites, Applied Mechanics Reviews 56 (2003) 215–230.
[12] Y. Jin, F.G. Yuan, Simulation of elastic properties of single-walled carbon nanotubes, Composites Science and Technology 63 (2003) 1507–1515.

[13] C. Li, T.W. Chou, Elastic moduli of multi-walled carbon nanotubes and the effect of van der Waals forces, Composites Science and Technology 63 (2003) 1517–1524.

[14] G.M. Odegard, V.M. Harik, K.E. Wise, T.S. Gates, Constitutive modeling of nanotube-reinforced polymer composites, Composites, Science and Technology 63 (2003) 1671–1687.

[15] M.B. Bryning, D.E. Milkie, M.F. Islam, J.M. Kikkawa, A.G. Yodh, Thermal conductivity and interfacial resistance in single-wall carbon nanotube epoxy composites, Applied Physical Letters 87 (2005) 161909; doi:10.1063/1.2103398.

[16] L. Gao, X. Zhou, Y. Ding, Effective thermal and electrical conductivity of carbon nanotube composites, Chemical Physics Letters 434 (4–6) (2007) 297–300.

[17] M.T. Strauss, R.L. Pober, Nanotubes in liquids: Effective thermal conductivity, Journal of Applied Physics 100 (8) (2006) 084328–084329.

[18] T.C. Clancy, T.S. Gates, Modeling of interfacial modification effects on thermal conductivity of carbon nanotube composites, Polymer 47 (16) (2006) 5990–5996.

[19] L. Xue, P. Keblinski, S.R. Phillpot, S.U.S. Choi, J.A. Eastman, Two regimes of thermal resistance at a liquid–solid interface, The Journal of Chemical Physics 118 (1) (2003) 337–339.

[20] Q.Z. Xue, Model for the effective thermal conductivity of carbon nanotube composites, Nanotechnology 17 (6) (2006) 1655–1660.

[21] S.T. Huxtable, D.G. Cahill, S. Shenogin, L. Xue, R. Ozisik, P. Barone, M. Usrey, M.S. Strano, G. Siddons, M. Shim, P. Keblinski, Interfacial heat flow in carbon nanotube suspensions, Nature of Materials 2 (11) (2003) 731–734.

[22] H. Zhong, J.R. Lukes, Interfacial thermal resistance between carbon nanotubes: Molecular dynamics simulations and analytical thermal modeling, Physical Review B (Condensed Matter and Materials Physics) 74 (12) (2006) 125403–125410.

[23] M. Foygel, R.D. Morris, D. Anez, S. French, V.L. Sobolev, Theoretical and computational studies of carbon nanotube composites and suspensions: Electrical and thermal conductivity, Physical Review B (Condensed Matter and Materials Physics) 71 (10) (2005) 104201–104208.

[24] S. Shenogin, L. Xue, R. Ozisik, P. Keblinski, D.G. Cahill, Role of thermal boundary resistance on the heat flow in carbon-nanotube composites, Journal of Applied Physics 95 (12) (2004) 8136–8144.

[25] S. Maruyama, Y. Igarashi, Y. Taniguchi, Y. Shibuta, Molecular dynamics simulations of heat transfer issues in carbon nanotubes, in: The 1st International Symposium on Micro & Nano Technology Honolulu, Hawaii, USA, 2004.

[26] S.U.S. Choi, Z.G. Zhang, W. Yu, F.E. Lockwood, E.A. Grulke, Anomalous thermal conductivity enhancement in nanotube suspensions, Applied Physics Letters 79 (14) (2001) 2252–2254.

[27] H.T. Zhu, C.Y. Zhang, Y.M. Tang, J.X. Wang, Novel synthesis and thermal conductivity of CuO nanofluid, Journal of Physical Chemistry C 111 (4) (2007) 1646–1650.

[28] X. Wang, X. Xu, S.U.S. Choi, Thermal conductivity of nanoparticle–fluid mixture, Journal of Thermophysics and Heat Transfer 13 (4) (1999) 474–480.

[29] S.J.V. Frankland, V.M. Harik, G.M. Odegard, D.W. Brenner, T.S. Gates, The stress–strain behavior of polymer–nanotube composites from molecular dynamics simulation, Composites Science and Technology 63 (2003) 1655–1661.

[30] P. Laborde-Lahoz, W. Maser, T. Martinez, A. Benito, T. Seeger, P. Cano, R. Villoria, A. Miravete, Mechanical characterization of carbon nanotube composite materials, Mechanics of Advanced Materials and Structures 12 (1) (2005) 13–19.

[31] D. Qian, G.J. Wagner, W.K. Liu, M.-F. Yu, R.S. Ruoff, Mechanics of carbon nanotubes, Applied Mechanics Reviews 55 (6) (2002) 495–533.

[32] K. Mylvaganam, L.C. Zhang, Important issues in a molecular dynamics simulation for characterising the mechanical properties of carbon nanotubes, Carbon 42 (10) (2004) 2025–2032.

[33] M. Griebel, J. Hamaekers, Molecular dynamics simulations of the elastic moduli of polymer–carbon nanotube composites, Computer Methods in Applied Mechanics and Engineering 193 (17–20) 2004 (2003) 1773–1788.

[34] V. Meunier, M.B. Nardelli, C. Roland, J. Bernholc, Structural and electronic properties of carbon nanotube tapers, Physical Review B 64 (19) (2001) 195419–195425.

[35] S.B. Legoas, V.R. Coluci, S.F. Braga, P.Z. Coura, S.O. Dantas, D.S. Galvão, Molecular-dynamics simulations of carbon nanotubes as gigahertz oscillators, Physical Review Letters 90 (5) (2003) 055504.

[36] A.K. Rappe, C.J. Casewit, K.S. Colwell, W.A. Goddard, W.M. Skiff, UFF, a full periodic table force field for molecular mechanics and molecular dynamics simulations, Journal of American Chemical Society 114 (25) (1992) 10024–10035.

[37] N. Yao, V. Lordi, Young's modulus of single-walled carbon nanotubes, Journal of Applied Physics 84 (4) (1998) 1939–1943.

[38] C.-W. Nan, R. Birringer, D.R. Clarke, H. Gleiter, Effective thermal conductivity of particulate composites with interfacial thermal resistance, Journal of Applied Physics 81 (10) (1997) 6692–6699.

[39] W. Jiajun, Y. Xiao-Su, Effects of interfacial thermal barrier resistance and particle shape and size on the thermal conductivity of AlN/PI composites, Composites Science and Technology 64 (10–11) (2004) 1623–1628.

[40] C.-W. Nan, Z. Shi, Y. Lin, A simple model for thermal conductivity of carbon nanotube-based composites, Chemical Physics Letters 375 (5–6) (2003) 666–669.

[41] C.-W. Nan, G. Liu, Y. Lin, M. Li, Interface effect on thermal conductivity of carbon nanotube composites, Applied Physics Letters 85 (16) (2004) 3549–3551.

[42] T. Mura, Micromechanics of Defects in Solids, Martinus Nijhoff, Hague, The Netherlands, 1997.